iScience

CellPress
OPEN ACCESS

Article

Detection of Lipase Activity in Cells by a Fluorescent Probe Based on Formation of Self-Assembled Micelles

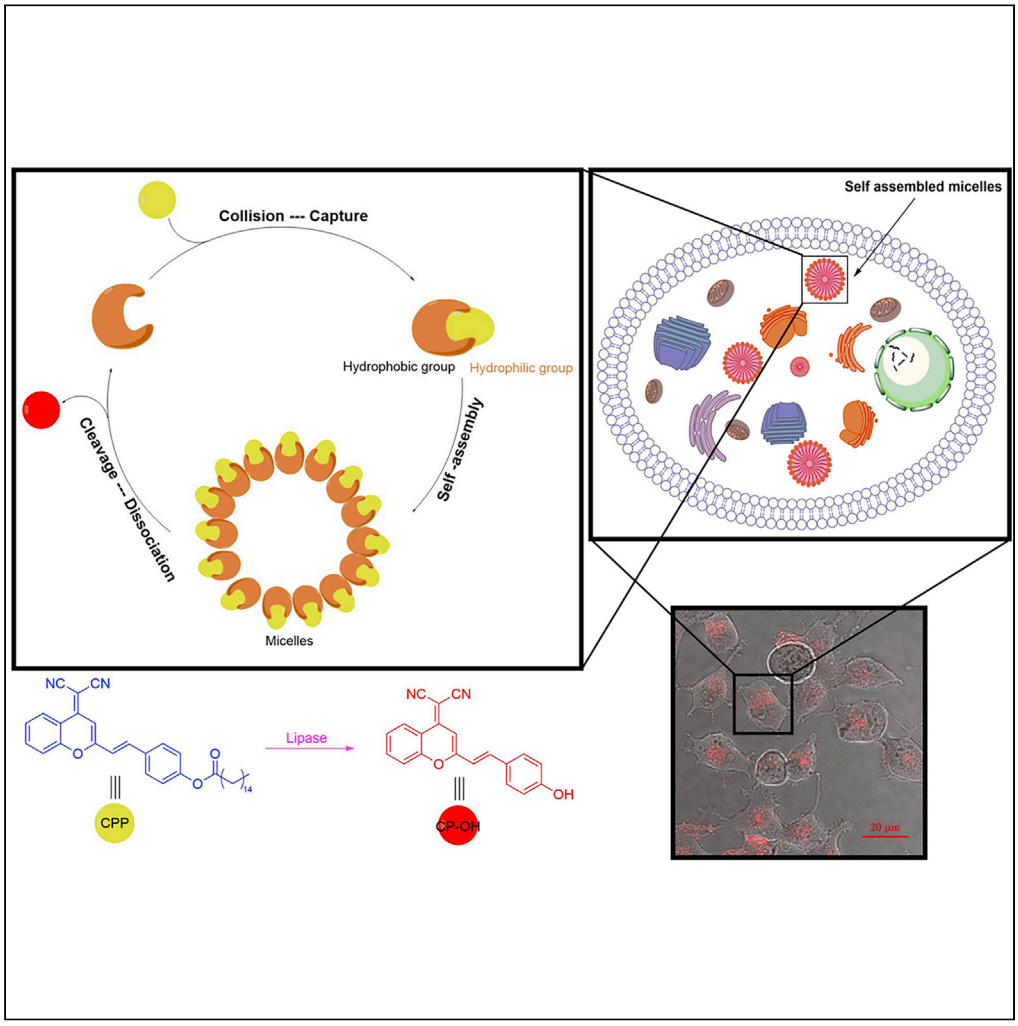

Zhen Qiao, Hongyi Zhang, Yanru Zhang, KeWei Wang

yanru.zhang@qdu.edu.cn (Y.Z.)
wangkw@qdu.edu.cn (K.W.)

HIGHLIGHTS

A CPP probe is synthesized via acylation of fluorescent CP-OH and palmitoyl chloride

Hydrophobic CPP probe forms self-assembled micelles with hydrophilic lipase

The CPP selectively detects heterogeneous –catalysis of lipase activity in cells

The fluorescent CPP has developmental potential for diagnostic use in diseases

Qiao et al., iScience 23, 101294
July 24, 2020
https://doi.org/10.1016/j.isci.2020.101294

iScience

CellPress
OPEN ACCESS

Article

Detection of Lipase Activity in Cells by a Fluorescent Probe Based on Formation of Self-Assembled Micelles

Zhen Qiao,[1] Hongyi Zhang,[1] Yanru Zhang,[1,3,*] and KeWei Wang[2,3,4,*]

SUMMARY

Reliable and sensitive detection of lipase activity is essential for the early diagnosis and monitoring of acute pancreatitis or progression of digestive diseases. However, the available fluorescent probes for detection of lipase activity are only implemented in a hexane-water two-phase system due to the nature of heterogeneous catalysis of lipase, thus limiting their applications in direct imaging of lipase activity in living cells and tissues. Here we designed and synthesized a "turn on" fluorescent probe CPP based on self-assembled micelles for hydrolysis of lipase. The CPP probe exhibits high selectivity and excellent sensitivity for the detection of lipase in such a homogeneous system and is successfully applied for monitoring lipase activity in pancreatic AR42J cells, tissues, and serums. Taken together, the fluorescent CPP probe not only provides a tool for diagnostic potential in pancreatic disease but also demonstrates an application potential for micelle self-assembly-based development of biological probes.

INTRODUCTION

Lipase is secreted into the small intestine where it hydrolyzes triglycerides into glycerol and fatty acids, performing an essential role in the digestive function (Carriere et al., 1993). Inactivation of lipase in mammals can increase adipose mass, resulting in triacylglycerol deposition in multiple tissues and causing cardiac dysfunction (Kingsnorth et al., 1995; Wyncoll and Beale, 1998; Yoshida, 1993). As an important exocrine enzyme from pancreas, pancreatic lipase serves as an essential biomarker for early diagnosis and for monitoring the progress of acute pancreatitis (AP) (Catanzaro et al., 2016; Ignjatovic et al., 2000; Smith et al., 2005; Steinberg et al., 1985; Treacy et al., 2001; Yadav et al., 2002). AP is a common and severe inflammatory disease with high mortality despite treatment (Kononczuk et al., 2018). Therefore, development of convenient and sensitive assays for lipase activity *in vivo* is important and valuable for clinical use in the diagnosis of AP and other disorders such as obesity, pancreatic adenocarcinoma, and cardiac dysfunction (Liu et al., 2006; Nawimanage et al., 2017; Shi et al., 2017a).

The conventional methodology for detection of lipase activity, such as acid-base titration and colorimetric analysis, requires the extraction of lipase from cells or tissues and renders drawbacks including damage of lipase activity due to the alteration of native enzymatic environment and a large error between measurements and actual values. In addition, these methods undergo complex sample processing and instrumental procedures, which are unsuitable for *in situ* monitoring of lipase activity (Gill et al., 2006; Kim et al., 2011; Peng et al., 2014; Teng et al., 2015; Wu et al., 2016; Yan et al., 2012; Yin et al., 2017; Zhang et al., 2013). To overcome those obstacles, fluorescent probes have recently received widespread attention owing to their high sensitivity, convenience, rapid implementation, noninvasiveness for imaging, and simplicity in preparations of biological samples (Glembockyte et al., 2018; Gou et al., 2018; Gurram et al., 2018; Liu et al., 2019; Xiong et al., 2019; Yue et al., 2017; Zhang et al., 2018; Zhou et al., 2018). In the past, a few fluorescent probes for lipase activity have been developed based on aggregation-induced emission (Shi et al., 2017a, 2017b). These probes exhibit the advantages of high selectivity, low detection limit, and fast response to lipase but have the disadvantage of being implemented in two-phase system (hexane/PBS) in which the organic layer is separated for fluorescence measurements. This processing procedure is tedious, and the two-phase system also limits the application of these probes in cells and tissues (Shi et al., 2017a). To date, there is still an unmet need for assays that can directly monitor the lipase activity *in vivo*. To realize the application of fluorescent probes *in vivo*, a challenge of developing a fluorescent

[1]Department of Medicinal Chemistry, Qingdao University School of Pharmacy, 308 Ningxia Road, Qingdao 266071, China

[2]Department of Pharmacology, Qingdao University School of Pharmacy, 308 Ningxia Road, Qingdao 266071, China

[3]Institue of Innovative Drug Discovery, Qingdao University, 38 Dengzhou Road, Qingdao 266021, China

[4]Lead Contact

*Correspondence: yanru.zhang@qdu.edu.cn (Y.Z.), wangkw@qdu.edu.cn (K.W.)

https://doi.org/10.1016/j.isci.2020.101294

probe with excellent performance in a homogeneous phase has to be met because lipase as a heterogeneous catalytic enzyme has the best catalytic activity at the oil-water interface (Reis et al., 2009).

The Michaelis-Menten-Henri kinetic model describes short- and medium-chain lipids that are favorable to interfacial hydrolysis by lipase, because they are solubilized into the aqueous phase and can easily break away from the interface to increase the "interfacial quality." Long-chain lipids are hydrolyzed by lipase to generate water-insoluble products that reorganize and aggregate on the surface of lipase, thus reducing the so-called interfacial quality and inhibiting the hydrolysis of long-chain lipids (Verger and De Haas, 1973). In water system, water-soluble acceptors of long-chain fatty acids such as β-cyclodextrin can improve the catalytic hydrolysis of long-chain lipids because these acceptors can remove water-insoluble long-chain fatty acids from the surface of lipase, enhancing the "interfacial quality" for maintaining catalytic activity of lipase (Reis et al., 2009). These observations suggest the feasibility of detecting lipase activity in a homogeneous system. A surfactant contains a polar head that is compatible with water and a hydrophobic unit compatible with oil. The amphipathic nature endows the interfacial characteristics of surfactants that can self-assemble to aggregates in diluted aqueous solutions to form micelles providing interfacial microenvironment (Drummond and Fong, 1999; Nagarajan and Ruckenstein, 1991). Therefore, we hypothesized that a hydrophobic probe and hydrophilic lipase can self-assemble to form micelles that allow the achievement of heterogeneous catalysis of lipase in a homogeneous phase.

To test this hypothesis, we designed and synthesized a "turn-on" fluorescent probe CPP (4-[2-[4-(dicyanomethylene)-4H-chromen-2-yl]vinyl] phenyl palmitate) with a long-chain saturated fatty acid palmitate that is hydrolyzed by lipase *in vivo*. Palmitate is commonly found in animals and vegetable fats in the form of glycerides and can enhance the biocompatibility between the CPP probe and lipase (Chapus; and Sémériva., 1976). The CPP probe exhibits an excellent response to lipase in a DMSO-water homogeneous system with self-assembled micelles formed by CPP and lipase. To the best of our knowledge, this is the first fluorescent probe developed and used for the detection of lipase activity in a homogeneous system. The CPP probe is characterized by high selectivity and excellent sensitivity without cytotoxicity, and it is successfully applied in the imaging of pancreatic AR42J cells and tissues in rats. Therefore, this CPP probe has developmental potential for diagnostic use in pancreatic function and diseases, and our findings also further advance the current understanding of catalytic reaction of lipase in a monophasic system.

RESULTS

Design and Synthesis of a Fluorescent Probe CPP for Detection of Lipase Activity in a Homogeneous System

The design of a fluorescent probe was based on our hypothesis that self-assembled micelles formed by hydrophilic lipase and hydrophobic probe can provide an interfacial microenvironment that allows heterogeneous catalysis of lipase in a homogeneous system. Palmitate is most commonly found in animal and vegetable fats in the form of glycerides and is hydrolyzed by lipase *in vivo*, indicating that it has ideal biocompatibility with lipase. The long alkyl chain of palmitate can have an easy access into the catalytic cavity of lipase because of its conformational flexibility. The fluorescence emission of 2-[2-(4-hydroxystyryl)-4H-chromen-4-ylidene] malononitrile (CP-OH) can be controlled by regulating the electron-donating ability of its hydroxyl. As the hydroxyl of CP-OH is protected by carboxylic acid group through ester bond, fluorescence emission will be quenched. When the hydroxyl is exposed by releasing carboxylic acid group, CP-OH will show strong fluorescence. This fluorescence regulatory mechanism is suitable for the detection of lipase activity because lipase is a specific enzyme for hydrolyzing esters into alcohols and fatty acids.

We started synthesizing a lipid-soluble fluorescent probe that combines palmitate as a recognition group for lipase and CP-OH as fluorophore. As shown in Scheme S1, the fluorophore CP-OH was prepared by the condensation reaction of 2-(2-methyl-4H-chromen-4-ylidene) malononitrile and 4-hydroxybenzaldehyde by catalysis of AcOH and piperidine in toluene. The CPP probe was synthesized via acylation reaction of CP-OH with palmitoyl chloride (Figures S1–S3). This lipid-soluble probe CPP can self-assemble into surfactant with lipase in homogeneous system as it interacts with lipase, thus forming micelles for heterogeneous catalytic reaction of lipase. The free probe CPP exhibits little fluorescence emission at 670 nm under excitation at 550 nm (Figure 1A). After incubation with lipase, the fluorescence emission at 670 nm appeared strongly upon excitation at 550 nm in DMSO-water homogeneous system. Meanwhile, the UV absorption spectra of CPP were measured in the same system. The probe CPP has no absorbance at 550 nm. As lipase was added into the CPP solution, the absorption peak at 550 nm increased obviously (Figure S4). The

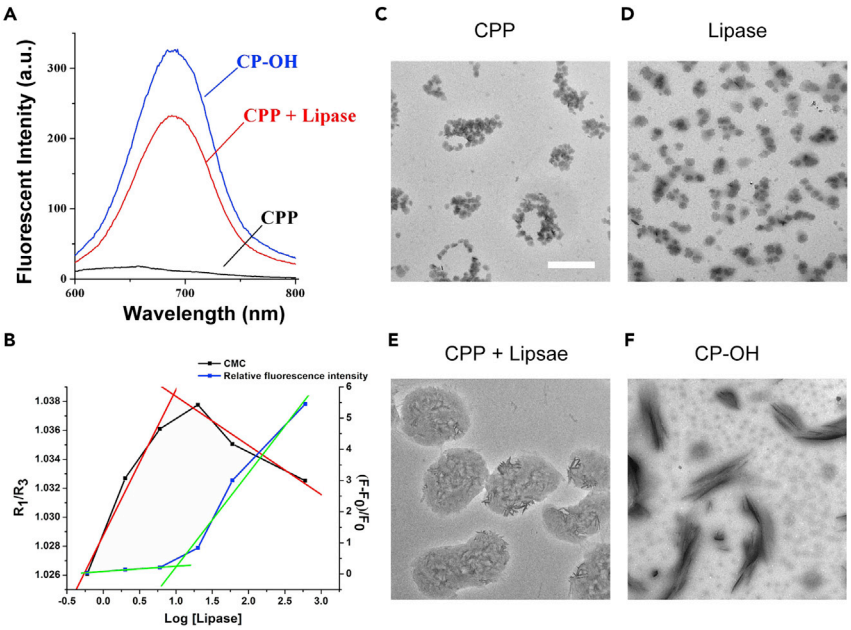

Figure 1. Fluorescent Spectrum, Critical Micelle Concentration, and TEM Images of Fluorescent Probe CPP

(A) Fluorescence spectra of CPP, CP-OH, and CPP + lipase under excitation at 550 nm.

(B–F) (B) Black curve: Fluorescence intensity ratio against the concentration of lipase with 10 μM CPP; R_1/R_3 represents the intensity ratios of pyrene at emission wavelengths 377 and 395 nm. The red curve was obtained by bilinear fitting, and the concentration of lipase (10 μg/mL) at the intersection point is the critical micelle concentration (CMC). Blue curve: Relative change of fluorescence intensity against the concentration of lipase with 10 μM CPP; F is the fluorescence of CPP with lipase, and F_0 is the fluorescence of free CPP. The green curve was obtained by bilinear fitting, and the intersection point of the two tangents indicates a dramatic increase of CPP fluorescence at concentration of lipase 10 μg/mL. Neither CPP (C) nor lipase (D) alone forms micelles; both CPPs and lipase (E) present in the DMSO-water solution can form the spherical aggregates with an average diameter about 1.5 μm; no spherical aggregates were observed in CP-OH (F) alone. Scale bar, 1 μm.

fluorescent and absorption spectra of fluorophore CP-OH were consistent with the product of CPP after incubation with lipase for 1 h, indicating the generation of CP-OH in CPP and lipase system. We further confirmed the generation of CP-OH in the homogeneous system (DMSO/PBS) by high-performance liquid chromatography (HPLC) (Figure S5).

Although there are a few reports on lipase-catalyzed synthesis in homogeneous system, the catalytic mechanism of lipase in homogeneous system still remains elusive (Monteiro et al., 2003). To verify the micelles formed by CPP and lipase, different concentrations (from 0.6 to 200 μg/mL) of lipase and CPP (10 μM) were mixed and the formation of micelles was detected by pyrene fluorescent probe under excitation at 334 nm. The fluorescence intensity of pyrene was monitored based on the ratio of emission wavelength at 377 nm to 395 nm for observation of critical micelle concentration (CMC). The CMC was generated under the condition of lipase at 10 μg/mL in tangent assay (Figure 1B black curve). To confirm that the formation of micelles provides a prerequisite for hydrolysis of lipase, we also detected the fluorescence of CPP for measurement of lipase. As shown by the blue curve in Figure 1B and by Figure S6, CPP fluorescence also increased at lipase concentration of 10 μg/mL, which was consistent with the generation of micelles. Similarly, dynamic light scattering analysis was performed at different concentrations of lipase with 10 μM CPP (Figure S7), revealing an increased average diameter of particles in the lipase and CPP mixture under the condition of 10 μg/mL lipase, likely through the formation of micelles between lipase and CPP. Taken together, these results indicated the formation of micelles between lipase and CPP, thus providing an interface for hydrolysis of CPP probe to release its CP-OH by heterogeneous catalysis of lipase.

In addition, we further examined the morphology of the micelles formed by lipase and CPP in DMSO-water solution using transmission electron microscopy (TEM). The CPPs or lipase alone in solution showed irregular aggregates (Figures 1C and 1D), indicating that neither lipid-soluble CPP nor water-soluble lipase was

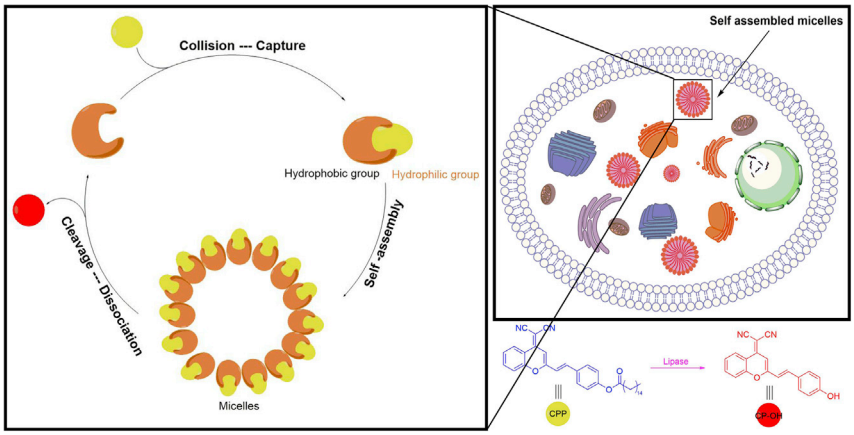

Figure 2. The Structure of Fluorescent Probe CPP and Its Proposed Detection Mechanism in DMSO/Water System

The free probe CPP without binding to lipase exhibits no fluorescent signal in DMSO/PBS system. Hydrophobic CPP was captured into the catalytic cavity of hydrophilic lipase via vigorous collision between the CPP and lipase in DMSO/PBS system. Hydrophobic CPP and hydrophilic lipase self-assemble into micelles. In the interfacial microenvironment, palmitate units are cut off to release palmitic acid and CP-OH by lipase-catalyzed cleavage of the ester bond in the probe CPP. The released CP-OH exhibits strong fluorescent signal after the dissociation from CPP via a catalytic reaction of lipase. The released lipases recapture new CPP to self-assemble into and restart the next catalytic cycle.

able to form micelles. In contrast, when both CPPs and lipase were present in the DMSO-water solution, the spherical aggregates were observed as solid cores with an average diameter about 1.5 μm (Figure 1E), a large structure of micelles formed by aggregation of surfactants (Ma et al., 2010). The relatively large vesicular micelles were likely due to the poor solubility of lipase in PBS, which resulted in the aggregation of lipase and CPPs to form self-assembled micelles in DMSO/PBS system (del Barrio et al., 2010; Park and Park, 2007). TEM examination further confirmed that the micelles were formed by aggregation of self-assembled surfactants from CPP and lipase, as compared with no spherical aggregates in DMSO/PBS solution of CP-OH (Figure 1F), providing an interface for heterogeneous catalysis of lipase to hydrolyze CPP into CP-OH in this homogeneous system.

In light of the fluorescence spectra and the morphology of CPP, CP-OH, lipase, and lipase + CPP, we proposed a detection mechanism that is illustrated in Figure 2. First, the free probe CPP shows undetectable fluorescence in the DMSO-water solution, because the hydroxyl of CP-OH is protected by a palmitate unit that suppresses the intramolecular charge transfer (ICT) by reducing the electron-donating ability of hydroxyl. Second, as CPP and lipase are dissolved in the DMSO-water system, the CPP probe and lipase are more prone to be present in the DMSO and water due to their lipid solubility and water solubility, respectively. Third, the intermiscibility of DMSO and water causes uninterrupted and vigorous collision between probe CPP and lipase. This vigorous collision and the excellent biocompatibility between palmitate and lipase caused an easy capture of the palmitate group of CPP by lipase. Thus, CPP and lipase can self-assemble into surfactants with CP-OH unit as the hydrophobic group and lipase as the hydrophilic group. These surfactants aggregate to form micelles, satisfying the requirement of interfacial catalysis. Finally, in such an interfacial microenvironment, palmitate units are cut off to release palmitic acid and CP-OH by lipase-catalyzed cleavage of the ester bond in the probe CPP. Meanwhile, the released CP-OH exhibits strong fluorescence emission centered at 670 nm owing to recovery of ICT effect resulting from the electron-donating ability of hydroxyl. The dissociated palmitic acid is solubilized into DMSO from micelles surface, and the micelles disintegrate to release lipases due to destruction of surfactants. The released lipases recapture new CPP to self-assemble into and restart the next catalytic cycle.

Fluorescence Spectroscopy of Probe CPP and Its Selectivity over Other Lipases and Amino Acids

The pH effect on probe CPP was tested at 37°C in DMSO/PBS (5:5, v/v) solution. Little fluorescence of CPP was observed in the pH range from 3 to 10 (Figure 3A), suggesting that probe CPP was stable at a wide pH

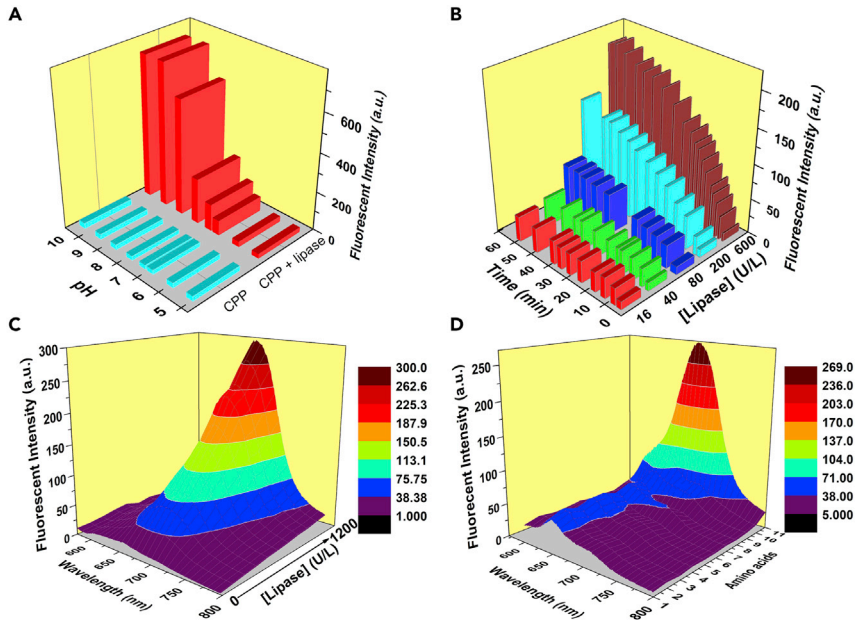

Figure 3. The Fluorescent Properties of Probe CPP and Its Selectivity Over Other Lipases and Amino Acids

(A) pH-dependent fluorescence intensity (670 nm) of CPP and CPP/lipase (600 U/L) in DMSO/PBS.

(B) Time-dependent fluorescence intensity of CPP with different concentration of lipase. Condition: [CPP] = 10 μM; DMSO:PBS, 5:5 v/v (pH = 7.4, 50 mM), and λ_{ex}, 550 nm (slit widths: 5 nm/10 nm).

(C) Fluorescence spectra of 10 μM CPP with the addition of lipase (0–1200 U/L) upon excitation at 550 nm in DMSO/PBS.

(D) Fluorescence spectra of (10 μM) CPP with lipases (6 mg/L, lipase from *Candida lipolytica* 100 U/mg) and amino acids (6 mg/L) upon excitation at 550 nm in DMSO/PBS. Lanes 1–11 are referred to CPP, L-leucine, L-arginine, L-glutamic acid, L-phenylalanine, L-cysteine, α-amylase, laccase, L-glutathione reduced, glucose oxidase, and lipase, respectively.

range. Upon addition of lipase, the fluorescence intensity at 670 nm upon excitation with 550 nm increased dramatically at pH range from 6 to 9 and reached a plateau at pH 9–10. These results indicated that alkaline condition accelerated the reaction of CPP converting to CP-OH in the presence of lipase. pH 7.4 was selected for further biological evaluation of the probe.

The time course of fluorescence from CPP (10 μM) was investigated under incubation of various activities of lipase (16–600 U/L) at 37°C for different period of time before fluorescence spectra were measured. The fluorescence emission at 670 nm increased obviously in 2 min, and the fluorescence intensity reached plateau within about 40 min (Figure 3B). These results indicated that CPP can rapidly respond to catalytic activity of lipase in both activity- and time-dependent manner.

To determine the relationship between lipase activity and fluorescence intensity detected by CPP probe, the titration was carried out in mixed solution of DMSO and PBS (5:5, v/v) at pH 7.4. As shown in Figure 3C, the fluorescence of free probe CPP (10 μM) was within the baseline level under excitation at 550 nm. Incubating with different concentrations of lipase at 37°C for 1 h resulted in activity-dependent increase of fluorescence intensity detected at 670 nm, exhibiting an excellent linearity between the fluorescence intensity and the activity of lipase from 0 to 280 U/L with a detection limit of 0.06 U/L (Figure S8). Because the normal range for serum lipase is within 0–60 U/L and abnormal lipase level in serum is usually greater than 180 U/L in the condition of AP, our assay with detection range from 0 to 280 U/L is likely suitable and robust for the early diagnosis of AP (Hofmeyr et al., 2014).

Selectivity is a crucial parameter for evaluation of a probe property. To evaluate the selectivity of CPP, the fluorescence emission spectra of CPP were measured in the presence of fixed concentration (6 mg/L) of CLL (lipase from *Candida lipolytica* at 100 U/mg) or different amino acids including leucine, arginine, glutamic acid, phenylalanine, cysteine, glucose oxidase, α-amylase, and laccase. As shown in Figure 3D, the fluorescence emission of CPP gave rise to an obvious peak at 670 nm upon addition of lipase (CLL). These

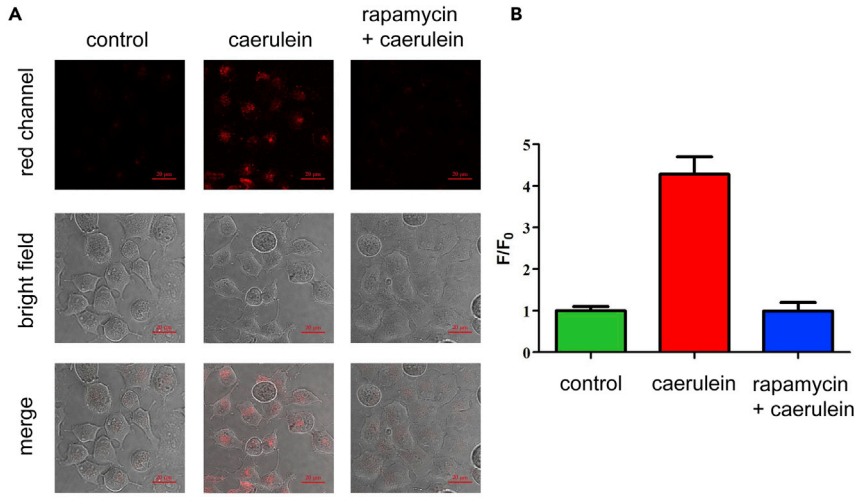

Figure 4. Live-Cell Imaging and Analysis of Pancreatic AR42J Cells in Single Photon

(A) Confocal fluorescence imaging (single-photon) and bright-field images of AR42J cells. In control group, cells were loaded with CPP (10 μM) for 60 min. In caerulein group, cells were loaded with CPP (10 μM) for 60 min before addition of caerulein (0.1 μM) for 12 h. In the rapamycin and caerulein group, cells were incubated with caerulein (0.1 μM) for 12 h, after being treated with inhibitor rapamycin (0.5 μM) for 0.5 h and before being loaded with CPP (10 μM) for 60 min.

(B) Relative change of fluorescence intensity detected by probe CPP under single-photon excitation. Excitation: 561 nm, and emission: 570–620 nm. F_0 is fluorescence intensity of AR42J cells loaded with CPP in control group, and F indicates fluorescence intensity of AR42J cells loaded with CPP after incubation with caerulein or rapamycin. Scale bar, 100 μm. The data are presented as the means ± SEM from three replicates (n = 3).

observations demonstrate that CPP can respond to lipase but not to other species, and the detection of lipase activity can be visualized by the color change.

Live Cell and Pancreatic Tissue Imaging of Endogenous Lipase by CPP

Caerulein is a 10-amino acid oligopeptide that stimulates pancreatic secretion of lipase through upregulation of intercellular adhesion molecule-1 protein of pancreatic acinar cells (Bonior et al., 2017; Yu et al., 2005). Using caerulein as a positive control, we performed confocal imaging of endogenous lipase by CPP in live pancreatic acinar (AR42J) cells. AR42J cells were incubated with caerulein (0.1 μM) for 12 h, and relative fluorescence intensity is counted as F/F_0 in AR42J cells. AR42J cells incubated with caerulein (0.1 μM) for 12 h showed strong fluorescence in single-photon channel when compared with vehicle control group (Figure 4). In contrast, rapamycin can inhibit the stimulatory effect of caerulein on AR42J cells leading to less lipase secretion (Nepomuceno et al., 2003). Therefore, we incubated AR42J with rapamycin (0.5 μM) for 0.5 h before stimulation with caerulein. Confocal imaging of AR42J cells exhibited reduced fluorescence in rapamycin-caerulein group. To further evaluate CPP capability for imaging endogenous lipase, CPP was used to detect the lipase level after incubation of caerulein for 6 and 12 h. The fluorescence intensity in 12-h group was stronger than that of the 6-h group (Figure S9), which was consistent with the literature report that caerulein-induced lipase level increases gradually with time (Yamaguchi et al., 1989). These results demonstrate that CPP can be used to detect endogenous lipase in living cells.

The co-localization of CPP with MitoTracker, ER-Tracker, or LysoTracker was performed to examine the subcellular organelle distribution of CPP in AR42J cells. As shown in Figure S10, red fluorescence CPP-associated spots are co-located with green spots corresponding to LysoTracker Green, indicating the distribution of probe CPP in lysosomes of AR42J cells. We further used the TEM assay to identify the generation of self-assembly micelles in cells. As shown in Figure 5, a substantial number of micelles were observed in the fractions F (cell-free extracts), N (nuclei), M (mitochondria, lysosomes, peroxisomes), and O (supernatant) of AR42J cells pre-incubated with CPP (10 μM) for 30 min, thus indicating the formation of intracellular micelles.

We also evaluated the cytotoxicity of CPP in AR42J cells using MTT assay. As shown in Figure S11, cell viability was not affected in the presence of CPP even at the high concentration (30 μM), indicating that probe CPP is unlikely to be liable for cytotoxicity in AR42J cells.

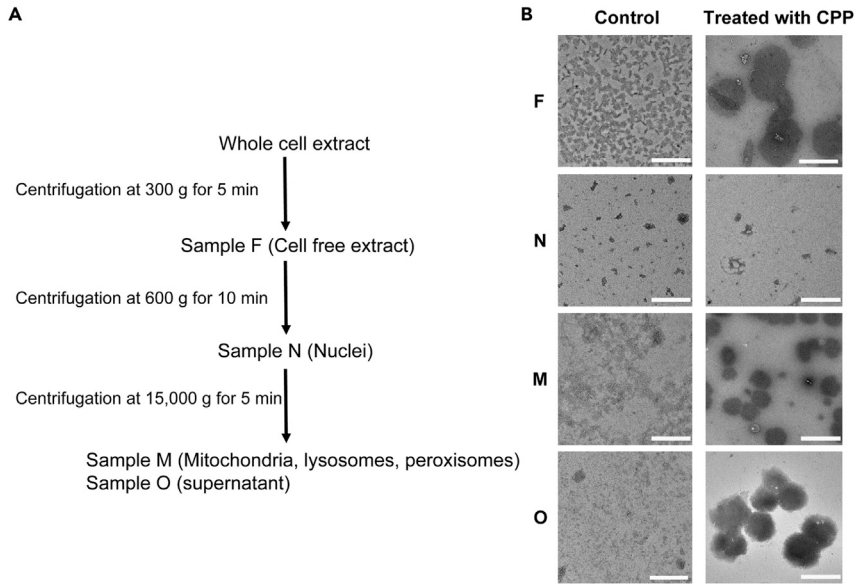

Figure 5. Method for the Separation of Cell Fractions, and the TEM Images of the Different Cell Fractions before and after Treatment with CPP

(A) Method of differential centrifugation for separation of cell fractions. Based on the reported protocol (Dopp et al., 2008), the fractions of AR42J cells were divided into four parts, named F (cell-free extracts), N (nuclei), M (mitochondria, lysosomes, peroxisomes), and O (supernatant) (Gao et al., 2012).

(B) The left column shows the morphology of each fraction of AR42J cells without treatment with CPP. The right column shows the morphology of each fraction of AR42J cells preincubated with CPP (10 μM) for 1 h. Scale bar, 1 μm.

We further applied the probe to detect lipase level in pancreatic tissues from normal rats and rats with AP induced by intraperitoneal injection of L-arginine (Guo et al., 2015; Liu et al., 2017). H&E staining was used to verify the success of L-arginine-induced AP. As shown in the control group, no acinar cell necrosis and hemorrhage were observed (Figure 6A left panel). In contrast, lobule outline damage with large areas of hemorrhage and necrosis and a large amount of inflammatory cell infiltration in the interstitium of pancreatic tissues were found in rats with AP (Figure 6A, right panel). These results indicated that rat model of AP induced by L-arginine was successful. We further used CPP and detected the lipase activity in pancreatic tissues from control rats or rats with AP. Confocal imaging through single-photon channel revealed that incubation with CPP (100 μM) at 37°C for 1 h resulted in a significant increase of fluorescence intensity in tissues from rats with pancreatitis, when compared with the control group (Figure 6B), indicating that CPP can penetrate the pancreatic tissues for direct detection of the lipase activity in rats with AP.

Detection of Exogenous and Endogenous Lipase in Mice Serum

To validate the application of CPP probe for detection of serum lipase, lipase activity was detected in serum samples supplemented with different concentrations (0–1,600 U/L) of exogenous lipase. As shown in Figure S12A, fluorescence intensity increased with increasing serum lipase activity under excitation at 550 nm. Incubating with different concentrations of lipase at 37°C for 1 h resulted in activity-dependent increase of fluorescence intensity detected at 650 nm, exhibiting an excellent linear relationship between the fluorescence intensity and lipase activity in the serum from 0 to 1,600 U/L (Figure S12B). Then, the CPP probe was utilized to detect the endogenous lipase activity in serum samples from normal mice or mice with AP induced by intraperitoneal injections of L-arginine. Equal volumes of CPP (20 μM in DMSO) were added into the serums before further incubation at 37°C for 1 h, and the fluorescence intensity was measured using fluorescence spectrophotometer. As shown in Figure S13, the fluorescence intensity in AP model group exhibited higher level than that in control group. These results suggested that probe CPP can be used to detect lipase in serum and may have developmental potential for clinical use in the diagnosis of pancreatitis.

In Vivo Visualization of Lipase

To test if CPP can be used for visualizing lipase in *vivo*, C57 mice were selected and divided into two groups. The first group was given an intraperitoneal injection of CPP as a control group, and no obvious

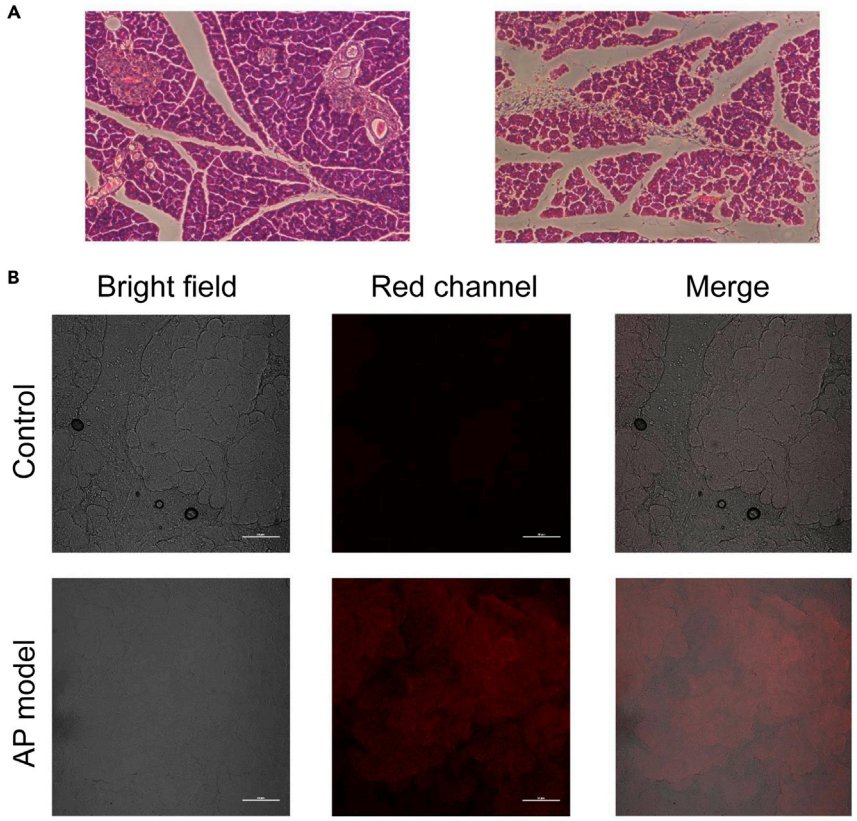

Figure 6. The H&E Staining and Fluorescence Imaging of Pancreatic Tissue

(A) Comparison of normal (left) and L-arginine-induced (right) pathological changes of rat pancreas.

(B) Tissue imaging of pancreas after incubation with CPP (100 μM) at 37°C for 1 h. Single-photon excitation: 561 nm, red channel collection: 570–620 nm. Scale bar, 100 μm.

fluorescence was detected. The other group was given intraperitoneal injections of lipase and then the probe CPP, and a strong fluorescence was observed (Figure S14). These results demonstrate the feasibility of application of CPP for visualizing the lipase in *vivo*.

DISCUSSION

In this study, we generated a "turn-on" fluorescent probe CPP for direct detection of lipase activity in a homogeneous phase (DMSO/PBS) using the combination of fluorescence, enzymatic reactions, and self-assembly. The TEM images of the cell fractions before and after incubation with CPP unambiguously identify the formation of the self-assembly micelles within the cells. We propose that the free probe CPP without fluorescence diffuses freely into cells due to its lipophilicity. In cells, hydrophobic CPP binds to the catalytic cavity of hydrophilic lipase and can self-assemble into micelles. In the interface of micelles, lipase catalyzes the hydrolysis of CPP to release CP-OH that exhibits a strong fluorescent signal. Thus, CPP can be used to detect lipase activity both in *vitro* and *vivo*. In addition, the self-assembled micelles can also serve as a foundation for detecting lipase activity in blood serum. The probe CPP exhibits the properties of high selectivity, outstanding sensitivity, and robust tissue penetration without obvious cytotoxicity. Our discovery of this probe CPP also demonstrates the feasibility of detecting heterogeneous catalytic enzyme in a homogeneous system.

Limitations of the Study

Although the lipase release upon micelle cleavage was confirmed using HPLC assay, a similar process in cells is yet to be demonstrated. The probe CPP is distributed in the lysosomes of AR42J cells, and super-high-resolution microscopy can be used to reveal the formation of self-assembled micelles in lysosomes. The faster response time for the fluorescent CPP probe can be further improved.

Resource Availability

Lead Contact

Further information and requests for resources and reagents should be directed to and will be fulfilled by the Lead Contact, KeWei Wang (wangkw@qdu.edu.cn).

Materials Availability

All unique/stable reagents generated in this study are available from the Lead Contact with a completed Materials Transfer Agreement.

Data and Code Availability

The published article includes all datasets generated during the study.

METHODS

All methods can be found in the accompanying Transparent Methods supplemental file.

SUPPLEMENTAL INFORMATION

Supplemental Information can be found online at https://doi.org/10.1016/j.isci.2020.101294.

ACKNOWLEDGMENTS

We would like to thank Mr. Jialiang Guan for the assistance in collection of pancreatic tissues and rat blood. The project is supported by the research grants awarded to K. Wang from the National Natural Science Foundation of China (NSFC81573410) and from Ministry of Science and Technology of the People's Republic of China (2018ZX09711001-004-006).

AUTHOR CONTRIBUTIONS

Z.Q. and H.Z. designed and carried out the experiments. Z.Q. drafted the manuscript. Y.Z. and K.W. supervised the project. Y.Z. and K.W. revised and finalized the paper.

DECLARATION OF INTERESTS

The authors declare no competing interest.

Received: November 18, 2019
Revised: May 25, 2020
Accepted: June 15, 2020
Published: July 24, 2020

REFERENCES

Bonior, J., Ceranowicz, P., Gajdosz, R., Kusnierz-Cabala, B., Pierzchalski, P., Warzecha, Z., Dembinski, A., Pedziwiatr, M., Kot, M., Leja-Szpak, A., et al. (2017). Molecular ghrelin system in the pancreatic acinar cells: the role of the polypeptide, caerulein and sensory nerves. Int. J. Mol. Sci. *18*, 929.

Carriere, F., Barrowman, J.A., Verger, R., and Laugier, R. (1993). Secretion and contribution to lipolysis of gastric and pancreatic lipases during a test meal in humans. Gastroenterology *105*, 876–888.

Catanzaro, R., Cuffari, B., Italia, A., and Marotta, F. (2016). Exploring the metabolic syndrome: nonalcoholic fatty pancreas disease. World J. Gastroenterol. *22*, 7660–7675.

Chapus;, C., and Sémériva, M. (1976). Mechanism of pancreatic lipase action. 2. Catalytic properties of modified lipases. Biochemistry *15*, 4988–4991.

del Barrio, J., Oriol, L., Sanchez, C., Serrano, J.L., Di Cicco, A., Keller, P., and Li, M.H. (2010). Self-assembly of linear-dendritic diblock copolymers: from nanofibers to polymersomes. J. Am. Chem. Soc. *132*, 3762–3769.

Dopp, E., von Recklinghausen, U., Hartmann, L.M., Stueckradt, I., Pollok, I., Rabieh, S., Hao, L., Nussler, A., Katier, C., Hirner, A.V., et al. (2008). Subcellular distribution of inorganic and methylated arsenic compounds in human urothelial cells and human hepatocytes. Drug Metab. Dispos *36*, 971–979.

Drummond, C.J., and Fong, C. (1999). Surfactant self-assembly objects as novel drug delivery vehicles. Curr. Opin. Colloid Interface *4*, 449–456.

Gao, Y., Shi, J., Yuan, D., and Xu, B. (2012). Imaging enzyme-triggered self-assembly of small molecules inside live cells. Nat. Commun. *3*, 1033.

Gill, R., Freeman, R., Xu, J.P., Willner, I., Winograd, S., Shweky, I., and Banin, U. (2006). Probing biocatalytic transformations with CdSe-ZnS QDs. J. Am. Chem.Soc. *128*, 15376–15377.

Glembockyte, V., Wieneke, R., Gatterdam, K., Gidi, Y., Tampe, R., and Cosa, G. (2018). Tris -N-nitrilotriacetic acid fluorophore as a self-healing dye for single-molecule fluorescence imaging. J. Chem.Soc. *140*, 11006–11012.

Gou, Z., Zuo, Y., Tian, M., and Lin, W. (2018). Siloxane-based nanoporous polymers with narrow pore-size distribution for cell imaging and explosive detection. ACS Appl. Mater. Interfaces *10*, 28979–28991.

Guo, F., Zheng, S., Gao, X., Zhang, Q., and Liu, J. (2015). A novel acute necrotizing pancreatitis model induced by L-arginine in rats. Pancreas *44*, 279–286.

Gurram, B., Zhang, S., Li, M., Li, H., Xie, Y., Cui, H., Du, J., Fan, J., Wang, J., and Peng, X. (2018). Celecoxib conjugated fluorescent probe for identification and discrimination of cyclooxygenase-2 enzyme in cancer cells. Anal. Chem. *90*, 5187–5193.

Hofmeyr, S., Meyer, C., and Warren, B.L. (2014). Serum lipase should be the laboratory test of choice for suspected acute pancreatitis. S. Afr. J. Surg. *52*, 72–75.

Ignjatovic, S., Majkic-Singh, N., Mitrovic, M., and Gvozdenovic, M. (2000). Biochemical evaluation of patients with acute pancreatitis. Clin. Chem. Lab. Med. *38*, 1141–1144.

Kim, T.I., Park, J., Park, S., Choi, Y., and Kim, Y. (2011). Visualization of tyrosinase activity in melanoma cells by a BODIPY-based fluorescent probe. Chem. Commun. *47*, 12640–12642.

Kingsnorth, A.N., Galloway, S.W., and Formela, L.J. (1995). Randomized, double-blind phase II trial of lexipafant, a platelet-activating factor antagonist, in human acute pancreatitis. Br. J. Surg. *82*, 1414–1420.

Kononczuk, T., Lukaszuk, B., Miklosz, A., Chabowski, A., Zendzian-Piotrowska, M., and Kurek, K. (2018). Cerulein-induced acute pancreatitis affects sphingomyelin signaling pathway in rats. Pancreas *47*, 898–903.

Liu, X., Guo, X., Li, J., Wu, M., and Zhan, X. (2017). Interferon-gamma aggravated L-arginine-induced acute pancreatitis in sprague-dawley rats and its possible mechanism: trypsinogen activation and autophagy up-regulation. Pancreas *46*, 619–625.

Liu, Y., Niu, J., Wang, W., and Lin, W. (2019). Tracking of mitochondrial endogenous ribonucleic acid in the cancer cells and macrophages using a novel small-molecular fluorescent probe. Anal. Chem. *91*, 1715–1718.

Liu, Z., Dai, J., Dai, L., Deng, M., Hu, Z., Hu, W., and Liang, S. (2006). Function and solution structure of Huwentoxin-X, a specific blocker of N-type calcium channels, from the Chinese bird spider Ornithoctonus huwena. J. Bio. Chem. *281*, 8628–8635.

Ma, N., Li, Y., Ren, H.F., Xu, H.P., Li, Z.B., and Zhang, X. (2010). Selenium-containing block copolymers and their oxidation-responsive aggregates. Polym. Chem. *1*, 1609–1614.

Monteiro, J.B., Nascimento, M.G., and Ninow, J.L. (2003). Lipase-catalyzed synthesis of monoacylglycerol in a homogeneous system. Biotechnol. Lett. *25*, 641–644.

Nagarajan, R., and Ruckenstein, E. (1991). Theory of surfactant self-assembly: a predictive molecular thermodynamic approach. Langmuir *7*, 2934–2969.

Nawimanage, R.R., Prasai, B., Hettiarachchi, S.U., and McCarley, R.L. (2017). Cascade reaction-based, near-infrared multiphoton fluorescent probe for the selective detection of cysteine. Anal. Chem. *89*, 6886–6892.

Nepomuceno, R.R., Balatoni, C.E., Natkunam, Y., Snow, A.L., Krams, S.M., and Martinez, O.M. (2003). Rapamycin inhibits the interleukin 10 signal transduction pathway and the growth of Epstein Barr virus B-cell lymphomas. Cancer Res. *63*, 4472–4480.

Park, S.Y., and Park, M.H. (2007). The preparation and characterization of the cross-linked spherical, cylindrical, and vesicular micelles of poly(styrene-b-isoprene) diblock copolymers. Langmuir *23*, 6788–6795.

Peng, T., Wong, N.K., Chen, X., Chan, Y.K., Sun, Z., Hu, J.J., Shen, J., El-Nezami, H., and Yang, D. (2014). Molecular imaging of peroxynitrite with HKGreen-4 in live cells and tissues. J. Am. Chem. Soc. *136*, 11728–11734.

Reis, P., Holmberg, K., Watzke, H., Leser, M.E., and Miller, R. (2009). Lipases at interfaces: a review. Adv. Colloid Interface Sci. *147-48*, 237–250.

Shi, J., Deng, Q., Wan, C., Zheng, M., Huang, F., and Tang, B. (2017a). Fluorometric probing of the lipase level as acute pancreatitis biomarkers based on interfacially controlled aggregation-induced emission (AIE). Chem. Sci. *8*, 6188–6195.

Shi, J., Zhang, S., Zheng, M., Deng, Q., Zheng, C., Li, J., and Huang, F. (2017b). A novel fluorometric turn-on assay for lipase activity based on an aggregation-induced emission (AIE) luminogen. Sensors Actuat. B Chem. *238*, 765–771.

Smith, R.C., Southwell-Keely, J., and Chesher, D. (2005). Should serum pancreatic lipase replace serum amylase as a biomarker of acute pancreatitis? ANZ J. Surg. *75*, 399–404.

Steinberg, W.M., Goldstein, S.S., Davis, N.D., Shamma'a, J., and Anderson, K. (1985). Diagnostic assays in acute pancreatitis. A study of sensitivity and specificity. Ann. Intern. Med. *102*, 576–580.

Teng, Y., Jia, X., Li, J., and Wang, E. (2015). Ratiometric fluorescence detection of tyrosinase activity and dopamine using thiolate-protected gold nanoclusters. Anal. Chem. *87*, 4897–4902.

Treacy, J., Williams, A., Bais, R., Willson, K., Worthley, C., Reece, J., Bessell, J., and Thomas, D. (2001). Evaluation of amylase and lipase in the diagnosis of acute pancreatitis. ANZ J. Surg. *71*, 577–582.

Verger, R., and De Haas, G.H. (1973). Enzyme reactions in a membrane model. 1. A new technique to study enzyme reactions in monolayers. Chem. Phys. Lipids *10*, 127–136.

Wu, X., Li, L., Shi, W., Gong, Q., Li, X., and Ma, H. (2016). Sensitive and selective ratiometric fluorescence probes for detection of intracellular endogenous monoamine oxidase A. Anal. Chem. *88*, 1440–1446.

Wyncoll, D.L., and Beale, R.J. (1998). Prospective placebo-controlled randomized trial of lexipafant in predicted severe acute pancreatitis. Br. J. Surg. *85*, 279–280.

Xiong, K., Huo, F., Chao, J.B., Zhang, Y., and Yin, C. (2019). Colorimetric and NIR fluorescence probe with multiple binding sites for distinguishing detection of Cys/Hcy and GSH in vivo. Anal. Chem. *91*, 1472–1478.

Yadav, D., Agarwal, N., and Pitchumoni, C.S. (2002). A critical evaluation of laboratory tests in acute pancreatitis. Am. J. Gastroenterol. *97*, 1309–1318.

Yamaguchi, H., Kimura, T., Mimura, K., and Nawata, H. (1989). Activation of proteases in cerulein-induced pancreatitis. Pancreas *4*, 565–571.

Yan, S., Huang, R., Wang, C., Zhou, Y., Wang, J., Fu, B., Weng, X., and Zhou, X. (2012). A two-photon fluorescent probe for intracellular detection of tyrosinase activity. Chem. Asian J. *7*, 2782–2785.

Yin, C.X., Xiong, K.M., Huo, F.J., Salamanca, J.C., and Strongin, R.M. (2017). Fluorescent probes with multiple binding sites for the discrimination of cys, hcy, and GSH. Angew. Chem. Int. Ed. *56*, 13188–13198.

Yoshida, T. (1993). Gabexate mesilate in human acute pancreatitis. Gastroenterology *105*, 1922–1923.

Yu, J.H., Lim, J.W., Kim, K.H., Morio, T., and Kim, H. (2005). NADPH oxidase and apoptosis in cerulein-stimulated pancreatic acinar AR42J cells. Free Radic. Bio. Med. *39*, 590–602.

Yue, Y., Huo, F., Ning, P., Zhang, Y., Chao, J., Meng, X., and Yin, C. (2017). Dual-site fluorescent probe for visualizing the metabolism of cys in living cells. J. Am. Chem. Soc. *139*, 3181–3185.

Zhang, W., Li, P., Yang, F., Hu, X., Sun, C., Zhang, W., Chen, D., and Tang, B. (2013). Dynamic and reversible fluorescence imaging of superoxide anion fluctuations in live cells and in vivo. J. Am. Chem. Soc. *135*, 14956–14959.

Zhang, Z., Fan, J., Zhao, Y., Kang, Y., Du, J., and Peng, X. (2018). Mitochondria-accessing ratiometric fluorescent probe for imaging endogenous superoxide anion in live cells and Daphnia magna. ACS Sens. *3*, 735–741.

Zhou, E.Y., Knox, H.J., Reinhardt, C.J., Partipilo, G., Nilges, M.J., and Chan, J. (2018). Near-infrared photoactivatable nitric oxide donors with integrated photoacoustic monitoring. J. Am. Chem. Soc. *140*, 11686–11697.

iScience, Volume *23*

Supplemental Information

Detection of Lipase Activity in Cells by a Fluorescent Probe Based on Formation of Self-Assembled Micelles

Zhen Qiao, Hongyi Zhang, Yanru Zhang, and KeWei Wang

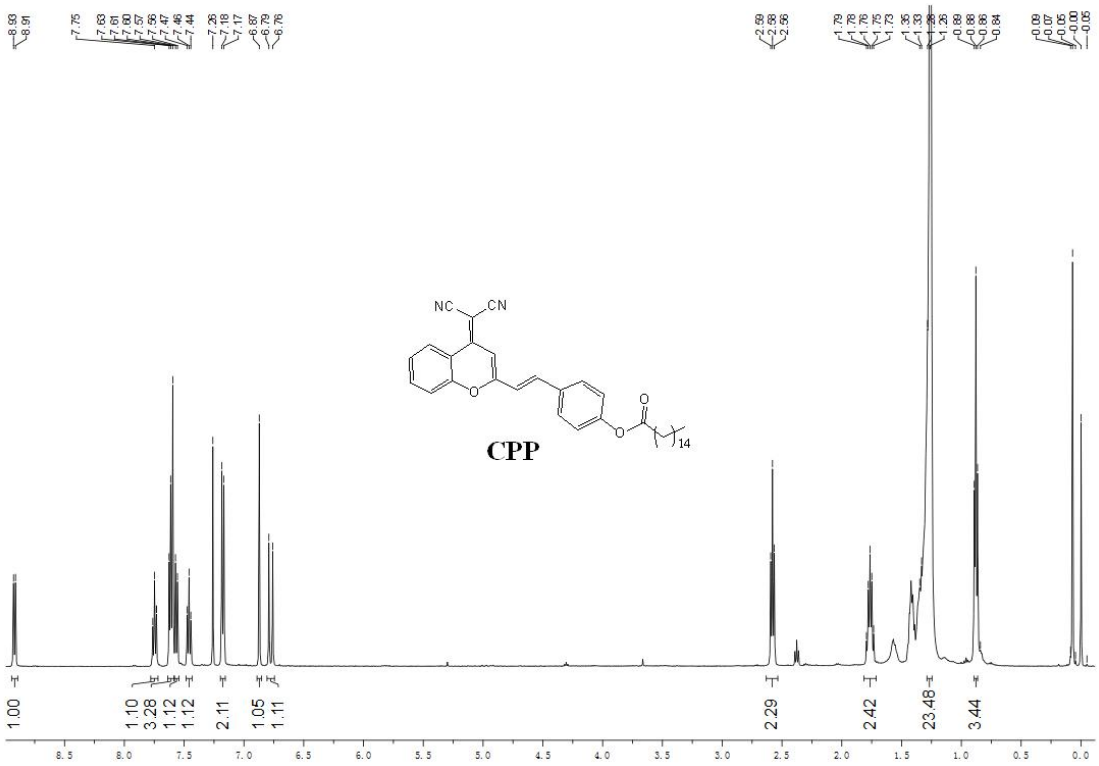

Figure S1. ^{1}H NMR Spectra of CPP. Related to Figure 1.

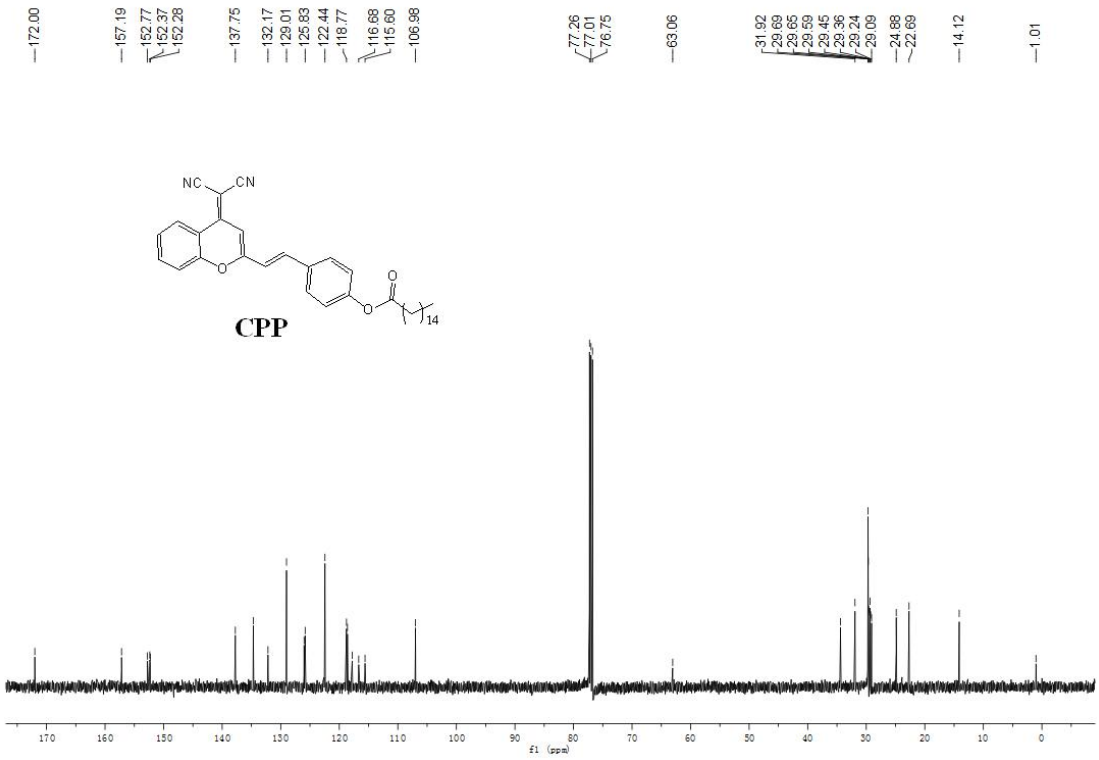

Figure S2. ^{13}C NMR Spectra of CPP. Related to Figure 1.

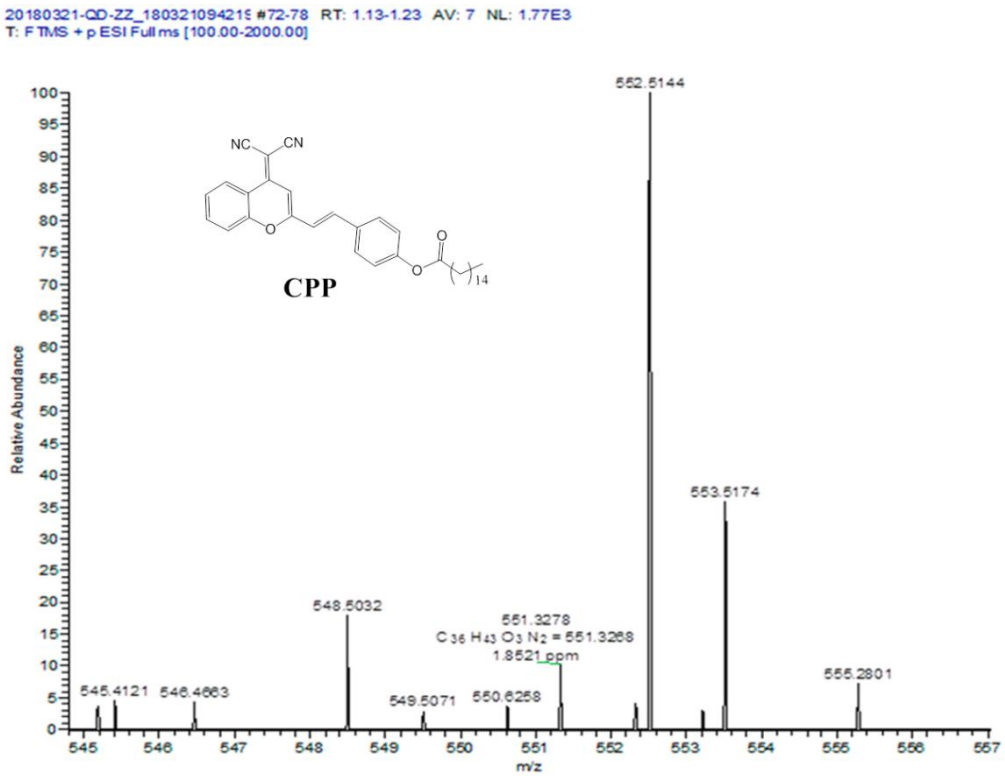

Figure S3. HRMS spectra of CPP. Related to Figure 1.

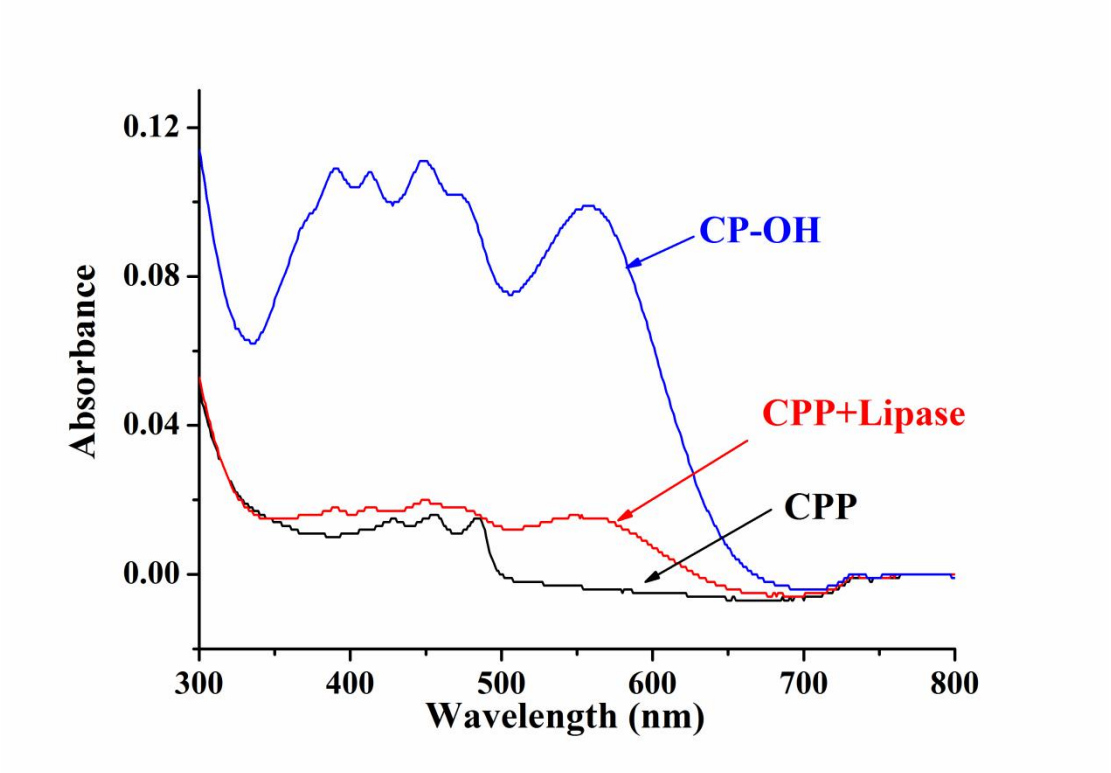

Figure S4. Absorption spectra of CP-OH, CPP + lipase and CPP. Related to Figure 1.

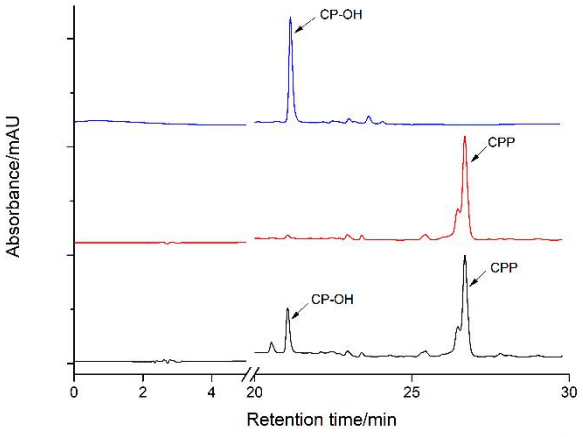

Figure S5. HPLC chromatograms of CPP (upper curve), CP-OH (mid curve) and CPP + Lipase (bottom curve). Related to Figure 1. 10% MeOH/H_2O to 100% MeOH, at 1 mL min^{-1} flow rate.

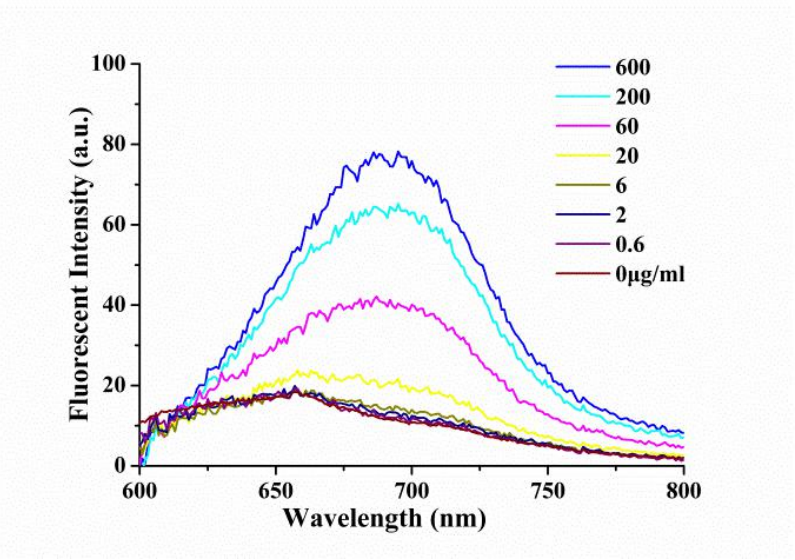

Figure S6. Fluorescent spectrum of CPP with different concentrations of lipase in Figure 1B blue curve. Related to Figure 1.

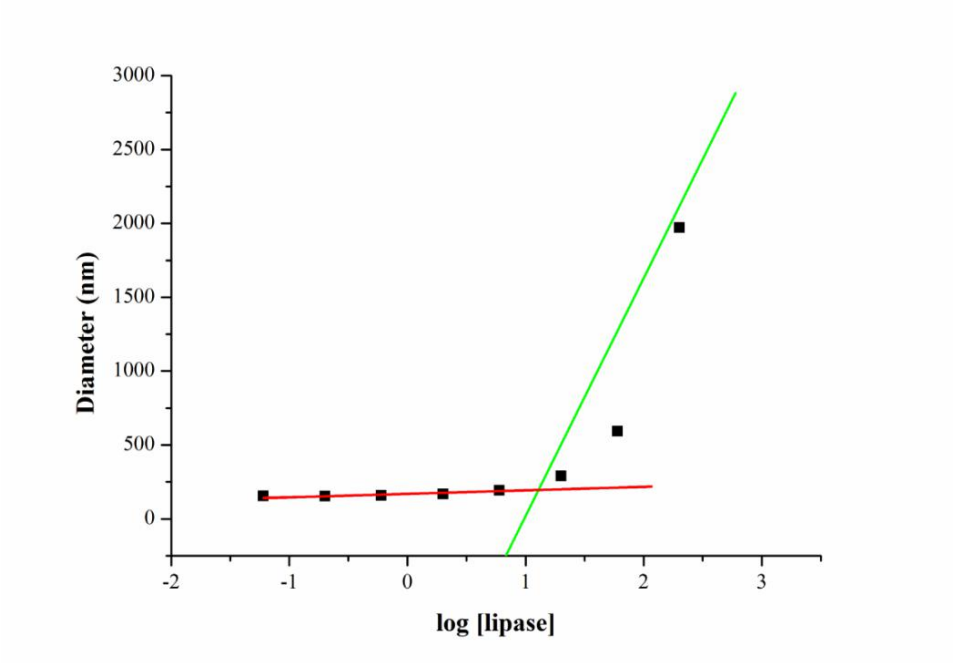

Figure S7. The particle size of 10 μM CPP in different concentrations of lipase in DMSO/PBS system. Related to Figure 1.

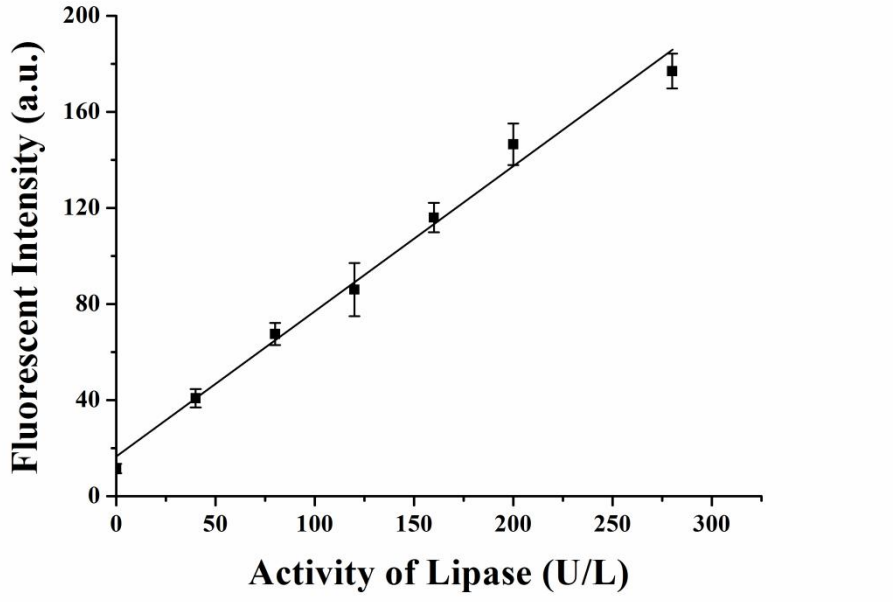

Figure S8. Linearity between the fluorescence intensity (670 nm) of CPP and activity of lipase. Related to Figure 3. Condition: [CPP] = 10 μM; DMSO: PBS (5:5, v/v, pH = 7.4, 50 mM), and λex: 550 nm (slit widths: 5 nm/10 nm). The data are presented as the means ± SEM from three replicates (n = 3).

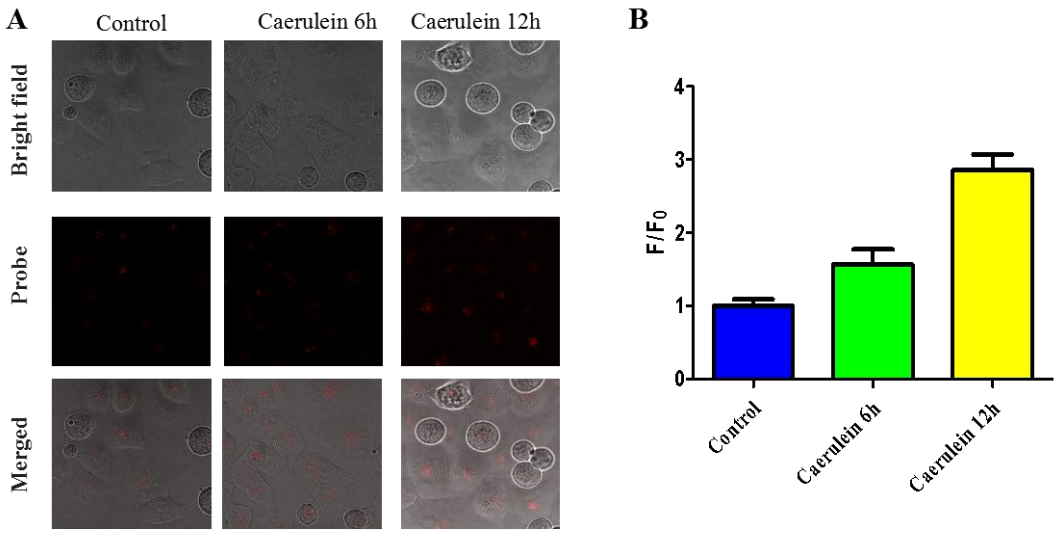

Figure S9. Fluorescence images and analysis of live AR42J cells under single-photon excitation. Related to Figure 4. (A) Confocal fluorescence and bright field images of AR42J cells. In control group, cells loaded with CPP (10 μM) for 60 min. In caerulein 6 h group, cells loaded with CPP (10 μM) for 60 min before addition of caerulein (100 nM) for 6 h. In caerulein 12 h group, cells loaded with CPP (10 μM) for 60 min before addition of caerulein (100 nM) for 12 h (B) Relative change of fluorescence-intensity detected by CPP. Where F_0 is fluorescence intensity of control group, F is fluorescence intensity of AR42J cells loaded with CPP after incubated with caerulein and rapamycin. Excitation: 561 nm, and red channel: 570 – 620 nm. Scale bar of 100 μm. Data are expressed as the means ± SEM with three replicates (n=3).

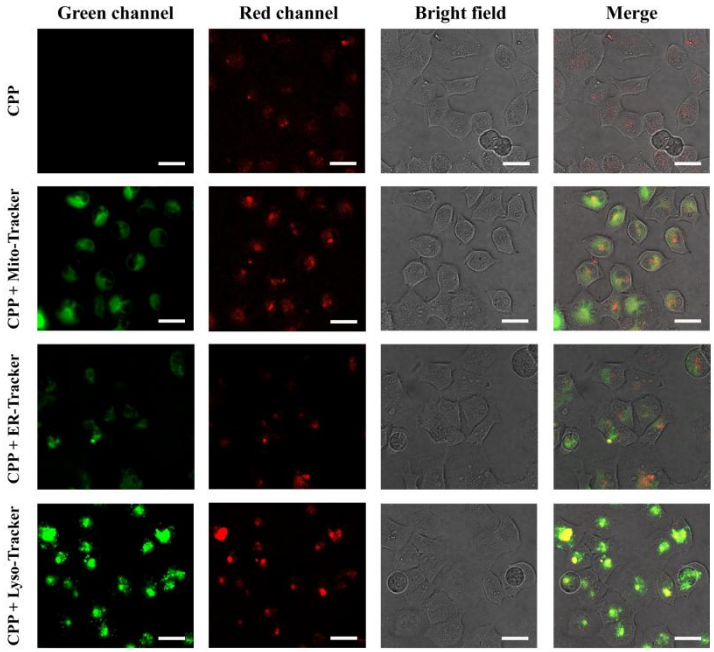

Figure S10. Confocal imaging of probe CPP in red channel and Mito Tracker or ER Tracker or Lyso Tracker in green channel in AR42J cells. Related to Figure 4. AR42J cells were incubated with probe CPP (10 μM) for 30 min, and then with Mito Tracker (200 nM) for 15 min or ER Tracker (2 μM) for 15 min or Lyso Tracker (50 nm) for 30 min.

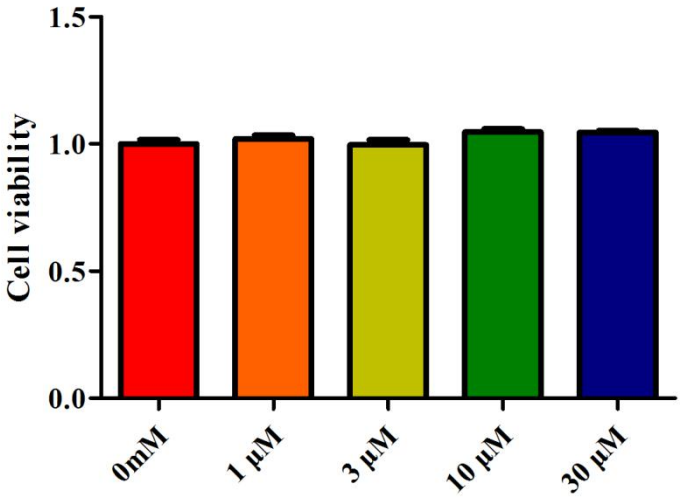

Figure S11. Cell viability of AR42J cells incubated with different concentrations of CPP. Related to Figure 4. The data are presented as the means ± SEM from three replicates (n = 3).

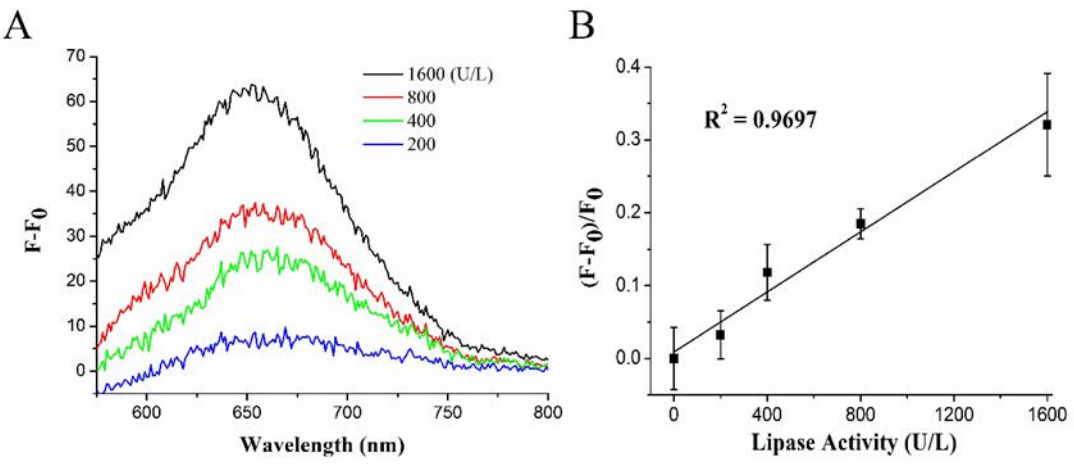

Figure S12. Linear correlation between exogenous lipase activity in serum and fluorescence intensity detected by CPP. Related to Figure 6. (A) Fluorescence spectra of CPP with different concentrations (0-1600 U/L) of serum lipase. F_0 is fluorescence intensity of serum without exogenous lipase after incubated with CPP (10 μM) at 37°C for 1 h; F is fluorescence intensity of serum loaded with different concentrations of exogenous lipase after incubated with CPP (10 μM) at 37°C for 1 h. (B) Linearity between the fluorescence intensity (650 nm) of CPP and serum lipase activity. Data are presented as the means ± SEM with 3 replicates.

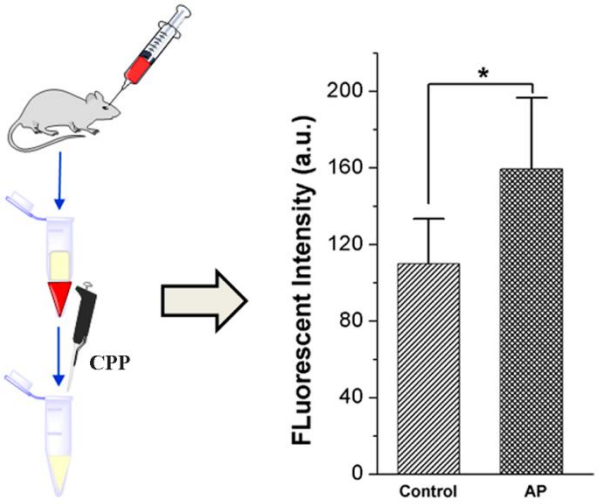

Figure S13. Measurement of fluorescence intensity change by CPP for serum lipase in mouse model of acute pancreatitis. **Related to Figure 6.** In control group, fluorescent intensity was measured after incubation of CPP and incubation at 37°C for 60 min. In acute pancreatitis (AP) group, mice were injected with L-arginin to induce acute pancreatitis. The data are expressed as the means ± SEM from three replicates (n = 5).

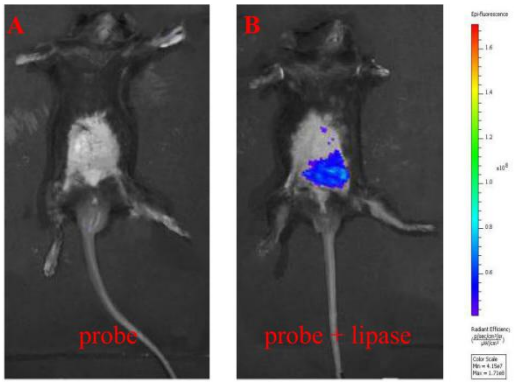

Figure S14. In *vivo* Fluorescent images of probe CPP in mice. Related to Figure 6.

(A) A mouse was given an injection of CPP only. (B) A mouse was given injections of lipase and then probe CPP.

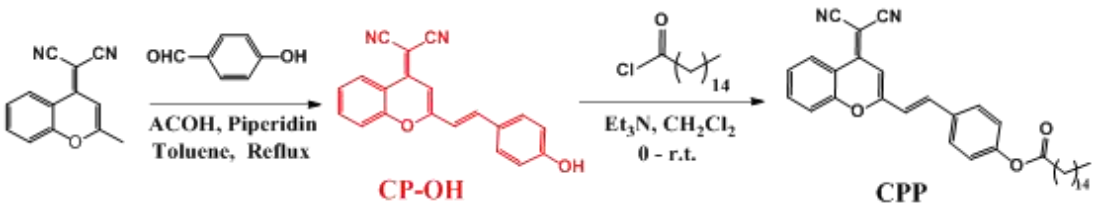

Scheme S1. The synthesis of CP-OH and CPP. Related to Figure 1.

Transparent Methods

Material and Apparatus

Unless otherwise stated, all reagents were purchased from Aladdin, Macklin, Sinopharm Chemical Reagent Co. and used without further purification. Twice-distilled water was used throughout all experiments. Lipase (PFL, CRL and CLL) and amino acids were purchased from Sigma-Aldrich. ^{1}H NMR (500 MHz) and ^{13}C NMR (125 MHz) spectra were acquired on a Bruker Avance-500 spectrometer, with $CDCl_3$ used as a solvent and tetramethylsilane (TMS) as an internal standard. HRMS spectra were obtained on a Q-TOF6510 spectrograph (Agilent). The absorbance of MTT was measured by microplate reader (Tecan Auatria GmbH A-5082). Fluorescent measurements were performed using F-4600 FL spectrophotometer. The confocal images of cells and tissues were captured by Nikon A1R MP. Quartz cuvettes with 1-mL volume were used for serum measurement, and cuvettes with a 1-cm path length and 3-mL volume were used for other measurements. The pH was determined with a pH meter (PHS-3C).

Synthesis of CPP

Compound CP-OH was synthesized based on the report by Liu et al (Fig. S1) (Wang et al., 2016). In brief, 2-(2-methyl-4H-chromen-4-ylidene) malononitrile (416 mg, 2 mmol) and 4-hydroxybenzaldehyde (305 mg, 2.5 mmol) were dissolved in toluene (40 mL). AcOH (0.5 mL) and piperidine (0.5 mL) were subsequently added into the mixture at room temperature. The mixture was refluxed under nitrogen protection for 10 h. After the reaction mixture was cooled to room temperature, the solvent was evaporated under reduced pressure, and the crude product was purified by column chromatography to yield red solid (368 mg, 58.9%).

Compound CP-OH (156 mg, 0.5 mmol) was dissolved in CH_2Cl_2 (25 mL) and triethylamine (2 mL). The mixture was cooled to 0°C before palmitoyl chloride (143 mg, 0.52 mmol) was dropwise added into the mixture at 0°C for 10 min. After the

reaction mixture as stirred at room temperature for 4 h, the solvent was removed under reduced pressure to obtain crude product. The crude product was purified by column chromatography to give yellow solid (144 mg, 52.4%). ^{1}H NMR (500 MHz, $CDCl_3$) δ 8.92 (d, *J* = 10 Hz, 1H), 7.75 (t, *J* = 7.5 Hz, 1H), 7.63–7.56 (m, 4H), 7.46 (t, *J* = 7.5 Hz, 1H), 7.17 (d, *J* = 5 Hz, 2H), 6.87 (s, 1H), 6.77 (d, *J* = 15 Hz, 1H), 2.58 (t, *J* = 7.5 Hz, 2H), 1.76 (m, 2H), 1.35–1.26 (m, 23H), 0.89–0.84 (t, 3H). ^{13}C NMR (125 MHz, $CDCl_3$) δ 172.00, 157.19, 152.77, 152.37, 152.28, 137.75, 132.17, 129.01, 125.83, 122.44, 118.77, 116.68, 115.60, 106.98, 63.06, 31.92, 29.69, 29.65, 29.59, 29.45, 29.36, 29.24, 29.09, 24.88, 22.69, 14.12, MS: m/z $[M+H]^+$ calcd for $C_{36}H_{43}N_2O_3$: 551.3278, found: 551.3274.

Cell Culture

Rat pancreatic exocrine cells, AR42J cells, were cultivated in Dulbecco's modified Eagle's medium (DMEM) with 10% fetal bovine serum (FBS) and 1% penicillin/streptomycin at 37°C in a 5% CO_2 condition.

Preparations of Cell Fractions for Transmission Electron Microscope (TEM)

AR42J cells were divided into two groups. Cells in control groups were only incubated with caerulein (0.1 μM) for 12h. Cells in experimental groups were incubated with caerulein (0.1 μM) for 12h and then treated with CPP (10 μM) for 1h at 37°C. Cells were washed three times with PBS, harvested by trypsin, and resuspended in PBS. Then, the cell suspensions were centrifuged at 300g for 5 min, and the obtained pellet was resuspended in 10 ml of distilled water for 30 min to break up the cells. Clumps of unbroken cells were removed by centrifugation at 300g for 5 min and sample F (cell free extracts) was obtained as supernatant. Sample F was centrifuged at 600g for 10 min to obtain Sample N (nuclei) as precipitate. Then the supernatant was centrifuged at 15,000g for 5 min to get sample O (supernatant) and sample M (Mitochondria, lysosomes, peroxisomes).

Fluorescence Spectroscopy

Probe CPP was dissolved in DMSO as stock solution (1 mM). Test solutions were prepared by diluting 100 μL of the stock solution into 10 mL mixture of phosphate buffer (0.05 M) and DMSO (5:5, V/V). Lipase (600U/L) was added, and the mixture solutions were shaken rigorously and incubated at 37°C for 1 h before recording of spectra using spectrophotometer.

Confocal Imaging of Lipase in Live Cells

The AR42J cells were randomly divided into six groups. Cells in control groups were incubated with PBS for 6 h or 12 h at 37°C in a 5% CO_2 condition. In caerulein groups cells were incubated with caerulein (0.1 μM) for 6 h or 12 h at 37°C in a 5% CO_2 condition. For inhibitor groups cells treated with inhibitor rapamycin (0.5 μM) for 0.5 h were added with caerulein (0.1 μM) for 6 h or 12 h at 37°C in a 5% CO_2 condition. AR42J cells were incubated with the probe (10 μM) for 1 h for fluorescence imaging under confocal fluorescence microscopy (Nikon A1R MP) with 40X objective, under the excitation with 561 nm for collection at 570-620 nm.

Cytotoxicity Test

About eight thousand AR42J cells were seeded in 96-well plate in 100 μL DMEM supplemented with 10% fetal bovine serum (FBS) and 1% penicillin/streptomycin at 37 ° C in a 5% CO_2 condition. Different concentrations of probe were added into 96-well plate for 24 h after overnight culture of AR42J cells. The 10 μL of MTT solution (5 mg/mL in PBS) was added into each well. After incubation at 37°C in a 5% CO_2 condition for 4 h, the previous medium was removed and 100 μL of DMSO were added into each well to dissolve the product for 1 h. Finally, the plate was placed in microplate reader (Tecan Auatria GmbH A-5082) for measurement of the absorbance at 492 nm. Each experiment was repeated at least three times.

Animals

Adult male Sprague-Dawley rats, C57 and Kunming mice were purchased from Beijing Vital River Laboratory Technology Co. Ltd (Beijing China). The animal experiment protocol was approved by the Animal Use and Care Committee of Qingdao University and according to the Ethical Guidelines of the International Association.

Pancreatic Tissue Imaging of Lipase in Rats

Rats were randomly divided into two groups (control group and L-Arg group). L-Arg group had three intraperitoneal (ip) injections of 100 mg/100 g weight of 20% L-arginine in 0.9% NaCl solution at an interval of an hour to induce acute pancreatitis (Guo et al., 2015; Liu et al., 2017). Control group had three i.p. injections of an equal volume 0.9% NaCl solution. After 12 hours of the last injection, rats were sacrificed to obtain pancreatic tissues for determination of pathological scores and tissue imaging. Pancreatic tissues of both control group and L-Arg group were incubated with the probe CPP (100 μM) for 1 h and washed three times with 0.9% NaCl for fluorescence imaging under a confocal fluorescence microscopy (Nikon A1R MP) with 20X objective, under the excitation with 561 nm for collection at 570-620 nm.

HE Staining

Pancreatic tissues were fixed in 4% paraformaldehyde for about 12 h before dehydrated with ethanol of gradient concentrations, and cleared in xylene and embedded in paraffin for final slicing into 5 μm thickness. After placed under a 37°C condition for 12 h, the slices were dewaxed in xylene and rehydrated with ethanol in gradient concentrations. Then slices were dyed by hematoxylin for about 5 min and quickly washed with 1% HCl in 70% ethanol. Thereafter, slices were covered by eosin for about 1 min and immersed in water for 20 min to remove the excess dye. After sealed by Neutral gum, the slices were examined for morphological changes of pancreatic tissues under light microscopy.

Fluorescent Imaging of Lipase in Living Mice

The C57 mice were used and abdominal fur was removed by electric shaver. Then the mice were divided into two groups. The control group of mice was given an intraperitoneal injection of CPP (100 μM, 200μL). The experimental group of mice was given an intraperitoneal injection of lipase (100 μg/ml, 200μL) and then the probe CPP (100 μM, 200μL). All the mice were anesthetized with 4% chloral hydrate before image. Finally, the mice were placed into the imaging chamber and imaged with the excitation at 550 nm and the emission at 670 nm.

CPP Detection of Exogenous Lipase in Mice Serum

C57 mice blood was drawn via ophthalmic vein, and the serum was obtained by centrifugation at 3,000 rpm/min for 5min. The serum was divided into five groups (100 μL) and added with different concentrations of lipase (0-1600 U/L) solution. The serum was further incubated with 1 ml CPP (10^{-5}M in DMSO and PBS 1:1) at 37°C for 1 h before measurement of fluorescence intensity by fluorospectrophotometer. Each experiment was repeated at least three times.

CPP Detection of Serum Lipase in Mouse Model of Acute Pancreatitis

The Kunming mice were randomly divided into two groups, control group and AP model group. The mice in AP model group had intraperitoneal (ip) injections of 20% arginine (200 mg/100 g) and the mice in control group had intraperitoneal (ip) injections of equal volume of 0.9% NaCl twice at intervals of 1 h for 12 h. The serums of these two groups were incubated with the probe at 37°C for 1h to measure fluorescence intensity by fluorospectrophotometer.

Supplemental References

Guo, F., Zheng, S., Gao, X., Zhang, Q., and Liu, J. (2015). A novel acute necrotizing pancreatitis model induced by L-arginine in rats. Pancreas *44*, 279-286.

Liu, X., Guo, X., Li, J., Wu, M., and Zhan, X. (2017). Interferon-gamma Aggravated L-Arginine-Induced Acute Pancreatitis in Sprague-Dawley Rats and Its Possible Mechanism: Trypsinogen Activation and Autophagy Up-regulation. Pancreas *46*, 619-625.

Wang, J.F., Li, B., Zhao, W.Y., Zhang, X.F., Luo, X., Corkins, M.E., Cole, S.L., Wang, C., Xiao, Y., Bi, X.M.*, et al.* (2016). Two-Photon Near Infrared Fluorescent Turn-On Probe Toward Cysteine and Its Imaging Applications. Acs Sensors *1*, 882-887.